

PROTON RESONANCE STUDY OF HYDRATED GALLIUM SULFATE

PROTON RESONANCE STUDY OF
HYDRATED GALLIUM SULFATE

By

DONALD WILLIAM KYDON, B.A.

A Thesis

Submitted to the Faculty of Graduate Studies

in Partial Fulfilment of the Requirements

for the Degree

Master of Science

McMaster University

November 1966

MASTER OF SCIENCE (1966)
(Physics)

McMASTER UNIVERSITY
Hamilton, Ontario.

TITLE: Proton Resonance Study of Hydrated Gallium Sulfate

AUTHOR: Donald William Kydon, B.A. (Johns Hopkins University)

SUPERVISOR: Professor H. E. Petch

NUMBER OF PAGES: vi, 39

SCOPE AND CONTENTS:

The nuclear magnetic resonance spectrum and the spin lattice relaxation time of protons in powdered hydrated gallium sulfate have been investigated and compared in order to determine the probable proton configurations.

The second moment and the relaxation time of the proton resonance were studied over a wide range of temperature. The NMR evidence is compatible with the existence of protons in OH^- and H_3O^+ configurations supporting the suggestion of Johansson (1962) based on an x-ray structure analysis.

ACKNOWLEDGEMENTS

I would like to thank Professor H. E. Petch for suggesting the topic of this thesis, for his guidance and encouragement offered throughout the course of the work.

Many thanks are due to Dr. M. Pintar for countless valuable discussions with him on the relaxation time experiment. I am also grateful to S. Vrscaj for his assistance in the details of the relaxation experiment.

The author received financial aid from McMaster University in the form of an assistantship. This research was made possible by grants-in-aid to Dr. Petch from the Defence Research Board of Canada.

TABLE OF CONTENTS

	PAGE
Introduction	1
(a) Nuclear Magnetic Resonance	1
(b) The Statement of the Problem	4
Theory	6
(a) Dipole-Dipole Interaction	6
(b) Molecular Reorientation as Revealed by the Resonance Linewidth	8
(c) Molecular Reorientation as Revealed by Transient Methods	11
Hydrated Gallium Sulfate	13
Apparatus and Experimental Arrangement	19
(a) Absorption Experiment	19
(b) Nuclear Spin-Lattice Relaxation Study	21
(c) The Effect of Inhomogeneities in H_1 and H_0	23
Experimental Procedure and Results	26
Discussion	36
Bibliography	39

LIST OF ILLUSTRATIONS

FIGURE		PAGE
1	Model for Nuclear Pair in Motion About Any Axis	9
2	Projection of Structure Along (010)	14
3	Projection of Structure Along (001)	15
4	Arrangement of Oxygen Atoms Around O_4	18
5	Block Diagram of the Absorption Spectrometer	20
6	Block Diagram of the T_1 Spectrometer	25
7	Absorption Derivative Curve at -268°C	27
8	Absorption Derivative Curve at $+22^\circ\text{C}$	28
9	Temperature Dependence of Second Moment	29
10	Photograph of Relaxation Signal at -138°C	31
11	Time Dependence of Induced Signal at -138°C	32
12	Temperature Dependence of T_1	33

LIST OF TABLES

TABLE		PAGE
I	Interatomic Distances	16
II	Tabulation of Results	34

INTRODUCTION

(a) Nuclear Magnetic Resonance

Nuclear Magnetic Resonance (NMR) is that phenomenon which is characterized by the emission or absorption of electromagnetic radiation associated with changes in the magnetic quantum number of certain nuclei in the presence of an applied magnetic field. Since its discovery (Purcell, Torrey and Pound; Bloch, Hansen and Packard) in 1945, NMR has developed into an effective technique for the study of the internal structure and properties of matter in the gaseous, liquid and solid states.

An atomic nucleus has an angular momentum \vec{J} and associated with it a magnetic moment $\vec{\mu}$. These are related by

$$\vec{\mu} = \gamma \vec{J}$$

where γ is a scalar called the gyromagnetic ratio. The above equation is often written

$$\vec{\mu} = g \left(\frac{e}{2Mc} \right) \vec{J}$$

where e = charge of proton

M = mass of proton

c = velocity of light, and

g = spectroscopic splitting factor.

The nuclear spin, denoted I , refers to the largest observable value of the component of \vec{J} in units of \hbar along any specified direction and is a pure number. The specified direction is usually along an applied magnetic field \vec{H} . In this case, the observable components of \vec{J} along \vec{H} are called J_H . Furthermore, the angular momentum and the spin

are related by

$$|J| = \hbar \sqrt{I(I+1)}$$

The components J_H are limited to discrete values given by

$$J_H = m \hbar$$

where m is the magnetic quantum number and restricted to $m = I, I-1, \dots, -(I-1), -I$.

The component of $\vec{\mu}$ along \vec{H} is

$$\begin{aligned} \mu_H &= g \left(\frac{e}{2Mc} \right) J_H = g \left(\frac{e}{2Mc} \right) \hbar m \\ &= g \mu_N m \end{aligned}$$

where $\mu_N = e\hbar/2Mc = 5.049 \times 10^{-24}$ erg/gauss is called the nuclear magneton.

In a magnetic field \vec{H} the magnetic moment precesses with the Larmor frequency

$$\omega_L = g \mu_N H / \hbar$$

and takes various discrete energies given by

$$E = -\vec{\mu} \cdot \vec{H} = -\mu_H H$$

Hence, there will be as many energy levels as there are possible components of $\vec{\mu}$ in the field direction. Transitions between these levels are governed by the magnetic dipole selection rule $\Delta m = \pm 1$. This implies that transitions are possible only between adjacent levels. It can easily be seen that resonance can occur when the oscillating magnetic field has an angular frequency ω such that,

$$\hbar\omega = \Delta E = g\hbar\mu_N H$$

and $\omega = \omega_L$, the Larmor frequency.

The g value for the proton is 5.58; hence, for a field of 10^4 gauss the resonance frequency is 42.5 Mc/sec. In general, resonance frequencies for various nuclei range from 1 Mc/sec. to more than 40 Mc/sec. for a field of 10^4 gauss.

Nuclear Magnetic Resonance yields information concerning many physical processes occurring in solids because the nuclei also interact with their neighbours. Such interactions affect the frequency, width, structure and temperature dependence of the resonance absorption. For example, neighbouring protons in a solid interact magnetically to produce an orientation-dependent broadening of the proton resonance. In certain solids, the molecular groups containing protons may reorient, when the temperature is sufficiently high, to produce some averaging of the orientation dependence. This makes it possible to detect these rotations or reorientations by studying the width of the resonance line as a function of temperature.

The processes of relaxation by which the nuclear spin system, having been disturbed by the oscillating field, returns to equilibrium with its surroundings are also important. When a material has been in a steady magnetic field for a sufficient length of time, more spins are aligned with the field than against it; in other words, there are more spins in the lower energy states. When an oscillating field at the resonance frequency is applied, some of its energy goes into flipping spins into higher energy states. Simultaneously, those spins which are

in higher energy states are stimulated by the oscillating field to flip to lower energy states with the emission of radiation. The strength of the absorption is determined, therefore, by the difference in occupation of the energy levels involved; if all levels were populated equally, the simultaneous effects of absorption and emission would cancel and no net absorption would be observed. However, since initially the lower levels are more densely populated (Boltzmann factor) a net absorption is observed. The strength of the absorption decays exponentially with time as a result of the approach toward the equalizing of populations which the absorption brings about. If the oscillating field is turned off for a time and then is turned back on, the strength of the absorption will be found to have grown or decayed as a result of the relaxation process. A measure of the time constant T_1 of decay or growth of the absorption gives information about the coupling of the spin system to its environment. The time constant T_1 is called the spin-lattice relaxation time. The lattice is taken here to mean all of the system except the nuclear spins. For solids, T_1 values lie within range 10^{-2} to 10^4 sec.

It should be noted also that nuclear spins are coupled to one another as well as to the lattice. This coupling leads to another kind of relaxation which is characterized by the time constant T_2 , the spin-spin relaxation time. The order of magnitude of T_2 in typical solids is 10^{-4} sec.

(b) The Statement of the Problem

The oxonium ion, H_3O^+ , has been known for some time to exist

in aqueous solutions. Also, crystal chemical considerations have led to the suggestion that this ion occurs in solids and NMR conductivity studies (Kakiuchi et. al., 1952; Shishkin, 1948) have provided some supporting evidence.

After solving the structure of hydrated gallium sulfate, $3\text{Ga}_2\text{O}_3 \cdot 4\text{SO}_3 \cdot 9\text{H}_2\text{O}$, using standard x-ray diffraction techniques, Johansson (1962) speculated that the water of hydration actually occurs partially as oxonium ions and that the structural formula should be written as $(\text{H}_3\text{O}^+) \text{Ga}_3(\text{OH})_6(\text{SO}_4)_2$. This suggestion is of more than intrinsic interest because it has bearing on a problem, basic in geochemistry, that the water of hydration in alunite, $\text{K}_2\text{O} \cdot 3\text{Al}_2\text{O}_3 \cdot 4\text{SO}_3 \cdot 6\text{H}_2\text{O}$, and isomorphous minerals is uncommonly variable. This phenomenon is not well understood yet but some acceptance has been given to the explanation that the variable water content is accommodated structurally by H_3O^+ replacement of the K^+ or equivalent ions (Shishkin, 1948). A meaningful study of alunite itself is difficult because a natural specimen is likely to have interfering impurities and the number of protons involved in H_3O^+ groups is likely to be only a small fraction of the total number of protons in the structure. Fortunately, the structure of hydrated gallium sulfate is so closely related to that of alunite that the same considerations as to the state of the water of hydration are likely to apply. Hence, information on hydrated gallium sulfate, itself providing an opportunity for a possible study of the H_3O^+ ions, will perhaps shed some light on the problem of variable water of hydration in the alunite-type minerals.

(a) Dipole - Dipole Interaction

The Hamiltonian operator for a system of N nuclear spins (this discussion is restricted to nuclei, $I = 1/2$) in a field \vec{H}_0 is:

$$H = H_0 + V$$

where $H_0 = -\sum_j g_j \mu_N I_{zj} \vec{H}_0$ represents the energy of the nuclear dipoles in a large external field \vec{H}_0 which is taken along the z direction. V is the dipole-dipole interaction term and is given by

$$V = \sum_{j>k} g_j^2 g_k^2 \mu_N^2 \left[\frac{\vec{I}_j \cdot \vec{I}_k}{r_{jk}^3} - 3(\vec{I}_j \cdot \vec{r}_{jk}) \frac{(\vec{I}_k \cdot \vec{r}_{jk})}{r_{jk}^5} \right] + \sum_{j,f} g_j g_f \mu_N^2 \left[\frac{\vec{I}_j \cdot \vec{I}_f}{r_{jf}^3} - \frac{3(\vec{I}_j \cdot \vec{r}_{jf})(\vec{I}_f \cdot \vec{r}_{jf})}{r_{jf}^5} \right]$$

In this equation \vec{r}_{jk} are the vectors connecting nuclei j and k, and r_{jk} is the magnitude of \vec{r}_{jk} . The subscripts j, k refer to resonating nuclei and the subscripts f refer to all other nuclear species in the sample.

To begin with, the use of this Hamiltonian in an attempt to calculate the shape of the absorption line in a completely general case presents an essentially impossible task. Only for a small number of interacting nuclei or for groups of nuclei displaying high symmetry is such a direct calculation feasible. However, Van Vleck (1948) showed that even in the general case it is possible to calculate the moments of the line shape. If $g(H)$ is the function describing the shape of the absorption line, then $(\Delta H)^n$ the n^{th} moment is given by

$$\overline{(\Delta H)^n} = \frac{\int_{-\infty}^{\infty} g(H) (H-H_0)^n dH}{\int_{-\infty}^{\infty} g(H) dH}$$

Of particular interest is the 2nd moment

$$\overline{(\Delta H)^2} = \frac{\int_{-\infty}^{\infty} g(H) (H-H_0)^2 dH}{\int_{-\infty}^{\infty} g(H) dH}$$

Usually, in a typical experiment the derivative of g with respect to H is measured rather than g itself. Hence, it is convenient to obtain an appropriate expression involving the derivative of g . Integrating by parts we get

$$\overline{(\Delta H)^2} = \frac{\frac{1}{3} \int_{-\infty}^{\infty} g'(H) (H-H_0)^3 dH}{\int_{-\infty}^{\infty} g'(H) (H-H_0) dH}$$

The value of the second moment may be written according to Van Vleck as

$$\overline{(\Delta H)^2} = \frac{3}{2} \frac{I(I+1)}{N} g^2 \mu_N^2 \sum_{j>k} \frac{(3 \cos^2 \theta_{jk} - 1)^2}{r_{jk}^6} + \frac{1}{3} \frac{\mu_N^2}{N} \sum_{j,f} I_f (I_f + 1) g_f^2 \frac{(3 \cos^2 \theta_{jf} - 1)^2}{r_{jf}^6}$$

where $g \mu_N I$ is the nuclear magnetic moment; the subscripts j, k refer to the nuclear species at resonance, the subscripts f refer to all other nuclear species in sample; N is the number of nuclei at resonance.

Often it is necessary to work with powdered samples where the orientation of r_{jk}, r_{jf} are distributed isotropically in space. In such a case, the factors $(3 \cos^2 \theta_{jk} - 1)^2$ and $(3 \cos^2 \theta_{jf} - 1)^2$ must be averaged over a sphere giving:

$$\overline{\Delta H^2} = \frac{6}{5} \frac{I(I+1)}{N} g^2 \mu_N^2 \sum_{j>k} \frac{1}{r_{jk}^6} + \frac{4}{15} \frac{\mu_N^2}{N} \sum_{j,f} \frac{I_f(I_f+1) g_f^2}{r_{jf}^6}$$

The above expressions for the values of the second moment for a single crystal and for a powder enable us to use the NMR method for the determination of certain structural parameters of a crystal.

(b) Molecular Reorientation As Revealed by the Resonance Linewidth

The effect of reorientation is indicated clearly by its influence upon the second moment. To include motion the factors $(3 \cos^2 \theta_{jk}' - 1)^2$ and $(3 \cos^2 \theta_{jf}' - 1)^2$ appearing in the second moment must be appropriately averaged.

Let us calculate the average for a rotation about any axis, (Fig. 1). The addition theorem for spherical harmonics yields

$$\overline{P_l(\cos \theta_{jk})}^\phi = P_l(\cos \theta') P_l(\cos \gamma_{jk})$$

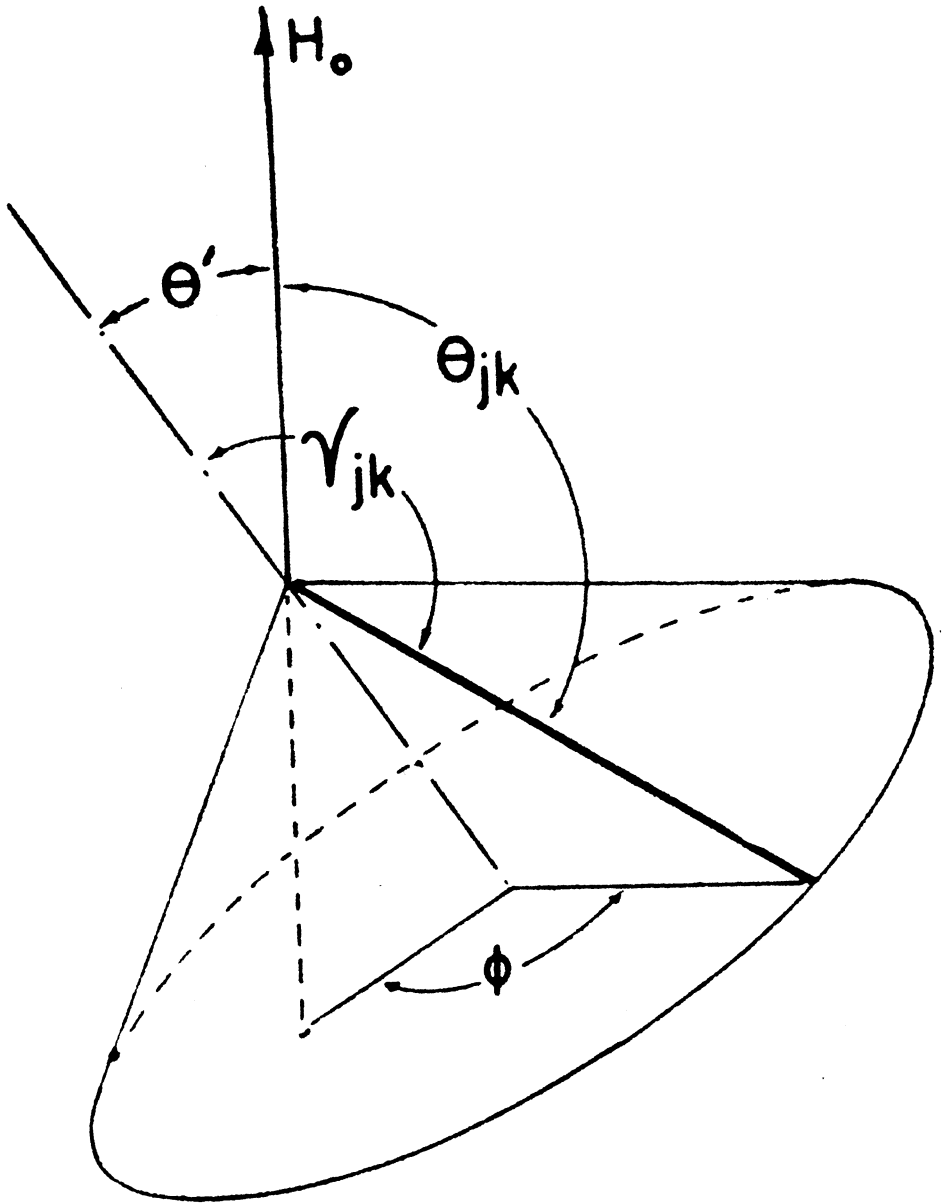
or for $l = 2$

$$\overline{3 \cos^2 \theta_{jk} - 1}^\phi = 1/2 (3 \cos^2 \theta' - 1) (3 \cos^2 \gamma_{jk} - 1)$$

and hence the second moment for a system rotating about axis making an angle θ' with H_0 is

$$\overline{\Delta H^2} = (3 \cos^2 \theta' - 1)^2 \left[\frac{3}{2} \frac{I(I+1)}{N} g^2 \mu_N^2 \sum_{j>k} \frac{3 \cos^2 \gamma_{jk} - 1}{r_{jk}^6} + \frac{1}{3} \mu_N^2 \sum_{j,f} \frac{I_f(I_f+1) g_f^2}{r_{jf}^6} (3 \cos^2 \gamma_{jf} - 1)^2 \right]$$

FIGURE 1**MODEL FOR NUCLEAR PAIR IN MOTION ABOUT ANY AXIS**



Model for a nuclear pair in motion

In powders we must again average over a sphere since the axes of rotation are randomly distributed.

$$\text{Hence } \overline{(3 \cos^2 \theta' - 1)^2} \text{ sphere} = \int_{\theta' = -\pi}^{\theta' = \pi} \frac{1}{4} (3 \cos^2 \theta' - 1)^2 \frac{\sin \theta' d\theta'}{2} = 1/5$$

and the second moment for a powder becomes

$$\overline{\Delta H^2} = 1/4 \left[\frac{6}{5} \frac{I(I+1)}{N} g^2 \mu_N^2 \sum_{j>k} \frac{(3 \cos^2 \gamma_{jk} - 1)^2}{r_{jk}^6} + \frac{4}{15} \frac{\mu_N^2}{N} \sum_{j,f} \frac{I_f(I_f+1) g_f^2 (3 \cos^2 \gamma_{jf} - 1)^2}{r_{jf}^6} \right]$$

If the rotational axis is normal to all internuclear vectors which contribute to the broadening then all γ_{jk} and γ_{jf} are $\pi/2$, it is then said that the second moment for a powder in which such rotation occurs is one-fourth as great as if the lattice were rigid.

Another important problem is the rate of reorientation necessary for observation of motional narrowing. Bloembergen et al. (1948) have shown that the narrowing process begins when the average period of reorientation approaches $1/2\pi\delta\nu$ where $\delta\nu$ is the line width on frequency scale. This theory introduces a quantity ν_c , the correlation frequency, defined as $\nu_c = 1/2\pi\tau_c$, where τ_c is correlation time. ν_c is the average rate at which significant changes occur in the atomic arrangement about a given nucleus. The motional narrowing can now be described by

$$(\delta\nu)^2 = (\delta\nu_0)^2 \frac{1}{2\pi} \tan^{-1} \delta\nu/\nu_c \quad (1)$$

where $(\delta\nu_0)$ is rigid lattice line width. A knowledge of the dependence

of ν_c on temperature gives the line narrowing as a function of temperature. In the event that the reorientation is thermally activated ν_c can be expressed as

$$\nu_c = \nu_{oc} \exp(-E_a/RT)$$

where E_a is the activation energy. From the NMR absorption a value of E_a can be derived by fitting (1) to the observed line width versus temperature curves. Furthermore, an estimate of the correlation frequency at the temperature where motion starts to influence the line width is obtained.

(c) Molecular Reorientation As Revealed by Transient Methods

If the reorientation process can be described by a single correlation time τ_c , the relationship between the spin relaxation time T_1 and τ_c should be of the form derived by Bloembergen et al. (1948)

$$\frac{1}{T_1} = C_1 \left[\frac{\tau_c}{1 + \omega^2 \tau_c^2} + \frac{4\tau_c}{1 + 4\omega^2 \tau_c^2} \right] \quad (2)$$

$\omega/2\pi$ = radio-frequency

$$C_1 = \frac{2}{5} \gamma^4 \hbar^2 I(I+1)/b^6 = \text{constant}; b = \text{nearest neighbour distance.}$$

The above expression is often referred to as the BPP formula.

If the molecular reorientation process is thermally activated and is governed by an activation energy E_a per mole, the variation τ_c with temperature should be

$$\tau_c = \tau_{oc} \exp(E_a/RT)$$

The procedure is to measure T_1 as a function of T . The value

of C_1 can be determined at the minimum value of T_1 (T_1 is minimum when $\omega\tau_c = 0.616$). If we restrict our attention to temperatures below that at which the minimum occurs and $\omega^2 \tau_c^2 \gg 1$, then we may write Equation 2

$$T_1 = 2\pi^2 \tau_{oc}^2 / C_1 v_L^2 \exp E_a / RT$$

A plot of $\log T_1$ against $1/T$ yields a straight line and E_a may be obtained from the slope without the need to use experimental values of T_1 near the minimum.

HYDRATED GALLIUM SULFATE

The structure of hydrated gallium sulfate, $3 \text{Ga}_2\text{O}_3 \cdot 4\text{SO}_3 \cdot 9\text{H}_2\text{O}$, was determined by George Johansson (1962) by x-ray methods. The crystal data are as follows:

System : hexagonal

Space group : $R\bar{3}m$

Cell dimensions: $a = 7.18\overset{\circ}{\text{A}}$, $c = 17.17\overset{\circ}{\text{A}}$, $V = 766\overset{\circ}{\text{A}}^3$

Cell contents : one formula weight in monoclinic unit cell

Projections of the structure along (010) and (001) are given respectively in Figures 2 and 3. Interatomic distances are listed in Table I. The structure is closely related to alunite, $\text{K}_2\text{O} \cdot 3 \text{Al}_2\text{O}_3 \cdot 4\text{SO}_3 \cdot 6\text{H}_2\text{O}$, and jarosite, $\text{K}_2\text{O} \cdot 3\text{Fe}_2\text{O}_3 \cdot 4\text{SO}_3 \cdot 6\text{H}_2\text{O}$, whose structures were solved by Hendricks (1937). In the gallium compound, however, the oxygen atoms occupy the positions of the potassium ions in the above mentioned compounds.

The gallium atoms are octahedrally surrounded by six oxygens. Two of these, O_2 , are at a distance of $2.02\overset{\circ}{\text{A}}$ and are each shared between one GaO_6 octahedron and one SO_4 tetrahedron. Four oxygens, O_3 , are at a distance of $1.95\overset{\circ}{\text{A}}$ and are each between the two GaO_6 octahedra. The O_3 atoms which are shared between two GaO_6 octahedra define a single oxygen bridge between the metal atoms.

Johansson suggested that probably the bridging oxygens, O_3 , are associated with one hydrogen atom each as this would increase the sum of the electrostatic bond strengths for these atoms from 1 to the expected value of 2. Each O_3 has, however, two oxygen atoms within hydrogen bonding distance. One is O_1 at a distance of $2.88\overset{\circ}{\text{A}}$; the other is O_4 at $2.82\overset{\circ}{\text{A}}$.

FIGURE 2
PROJECTION OF THE STRUCTURE ALONG [010]
(after Johansson)

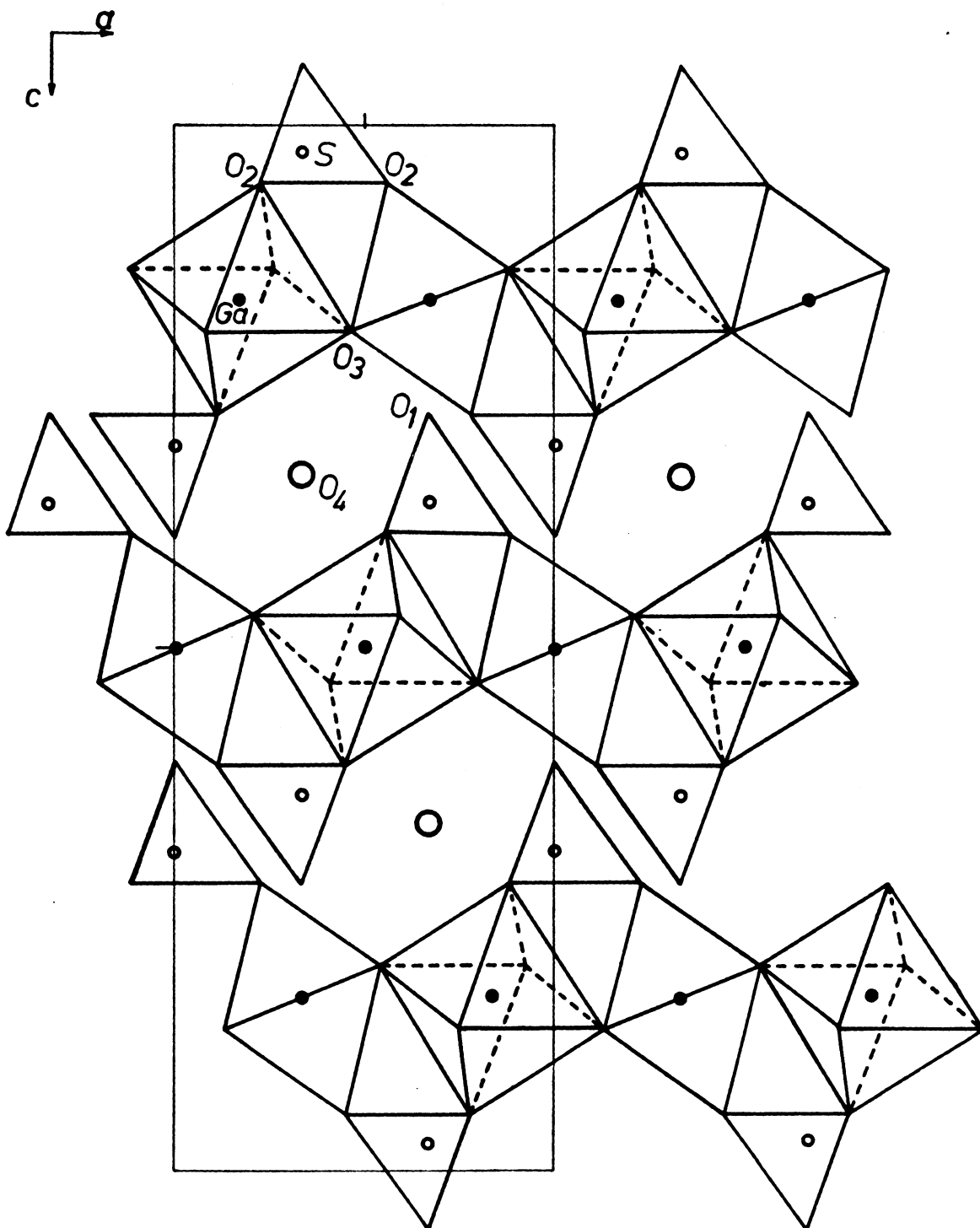
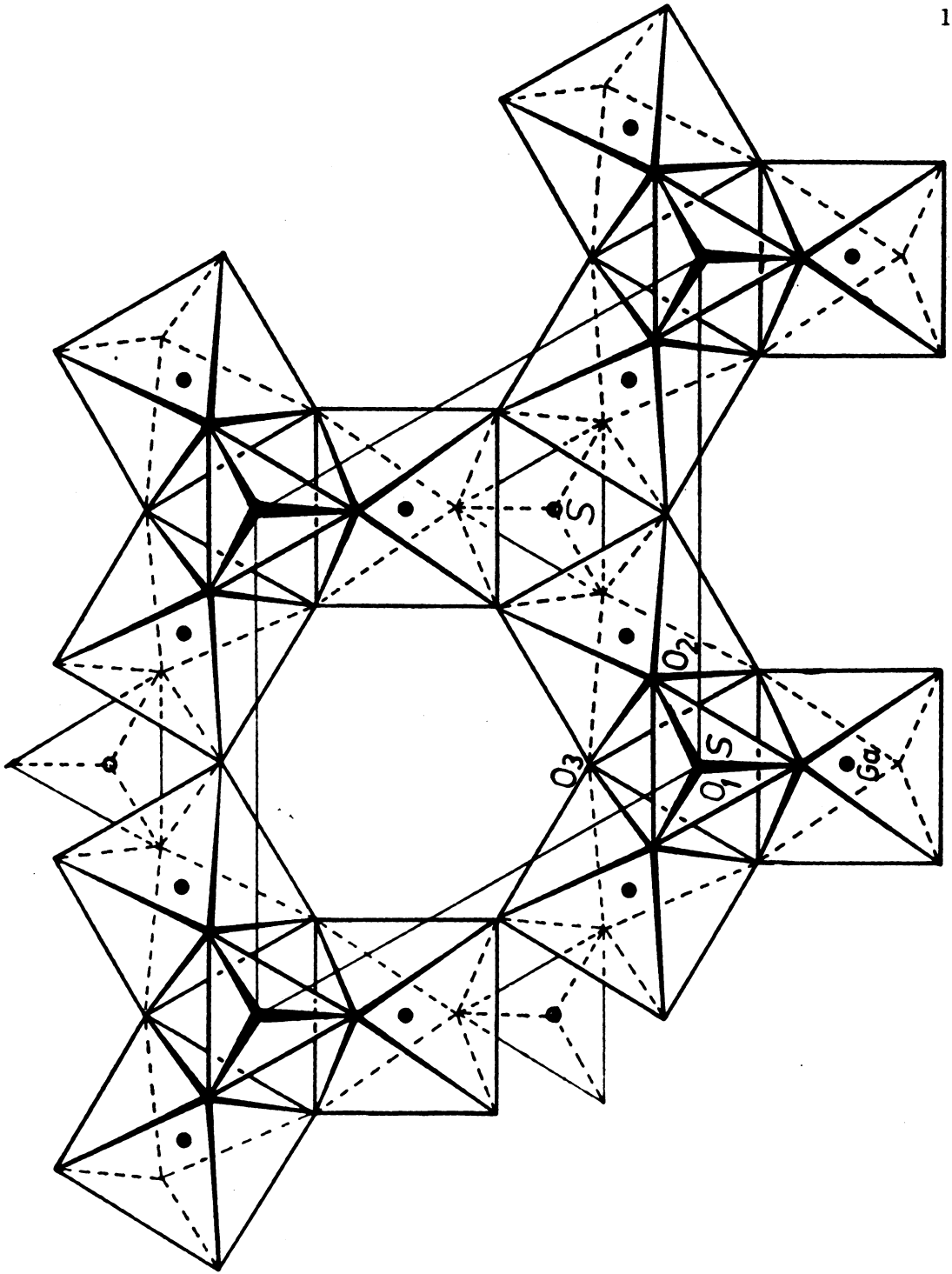


FIGURE 3
PROJECTION OF PART OF THE STRUCTURE ALONG [001]
(after Johansson)



Projection of part of the structure along [001].

TABLE I
INTERATOMIC DISTANCES

Within a GaO_6 octahedron:

$\text{Ga} - \overset{\circ}{\text{O}}_2$: 2.01 Å	$\overset{\circ}{\text{O}}_2 - \overset{\circ}{\text{O}}_3$: 2.86 Å
	2.75
$- \overset{\circ}{\text{O}}_3$: 1.95	$\overset{\circ}{\text{O}}_3 - \overset{\circ}{\text{O}}_3$: 2.75 Å
	2.77

Within an SO_4 tetrahedron:

$\text{S} - \overset{\circ}{\text{O}}_1$: 1.47 Å	$\overset{\circ}{\text{O}}_2 - \overset{\circ}{\text{O}}_2$: 2.41 Å
$- \overset{\circ}{\text{O}}_2$: 1.47	$- \overset{\circ}{\text{O}}_1$: 2.41

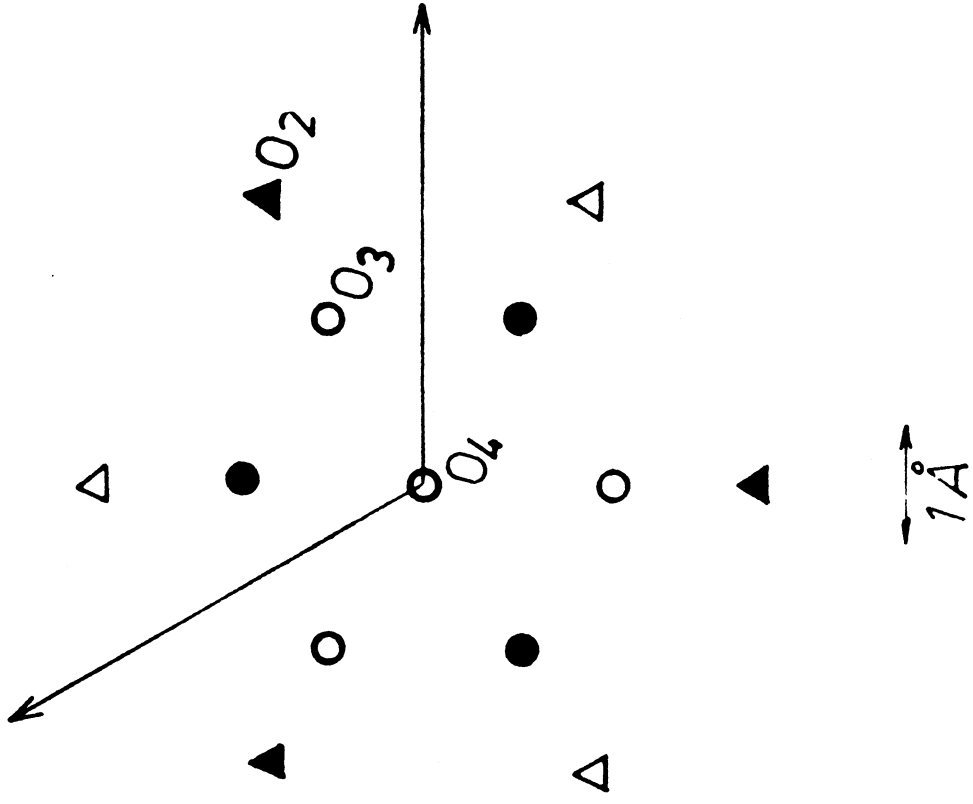
Other O - O distances < 3.5 Å:

$\overset{\circ}{\text{O}}_4 - \overset{\circ}{\text{O}}_2$: 2.92 Å	$\overset{\circ}{\text{O}}_2 - \overset{\circ}{\text{O}}_2$: 3.36 Å
$- \overset{\circ}{\text{O}}_3$: 2.82	$- \overset{\circ}{\text{O}}_3$: 3.49
$\overset{\circ}{\text{O}}_1 - \overset{\circ}{\text{O}}_3$: 2.88	

The positions of the oxygen atoms immediately surrounding O_4 are shown in Figure 4. There are six O_2 atoms at distances of 2.92A and six O_3 atoms at 2.82A. The short distances suggest that some type of hydrogen bonding interaction must occur. The symmetry around O_4 would seem to require that it is associated with three protons and that it should probably be a H_3O^+ ion. If O_4 were assumed to be a H_2O molecule, a more complicated kind of disorder or a lowering of the space group symmetry would have to be assumed.

Anhydrous gallium sulfate was obtained commercially. To obtain the alunite-related compound, the following hydrothermal synthesis was carried out. A solution 0.2 M in $Ga_2(SO_4)_3$ and 0.2 M in H_2SO_4 enclosed in a glass vehicle was placed in a stainless steel bomb. The bomb was then heated to 180°C for three days. Upon completion of the three-day hydrothermal treatment, the glass vehicle was removed. A white precipitate had formed. The precipitate was then mechanically separated from the remaining solution and left to dry for two days in a desiccator system. The polycrystalline sample was then ground up. At this point, a powder x-ray photograph was taken and the results checked with those of Johansson (1962).

FIGURE 4
THE ARRANGEMENT OF OXYGEN ATOMS AROUND O_4
(after Johansson)



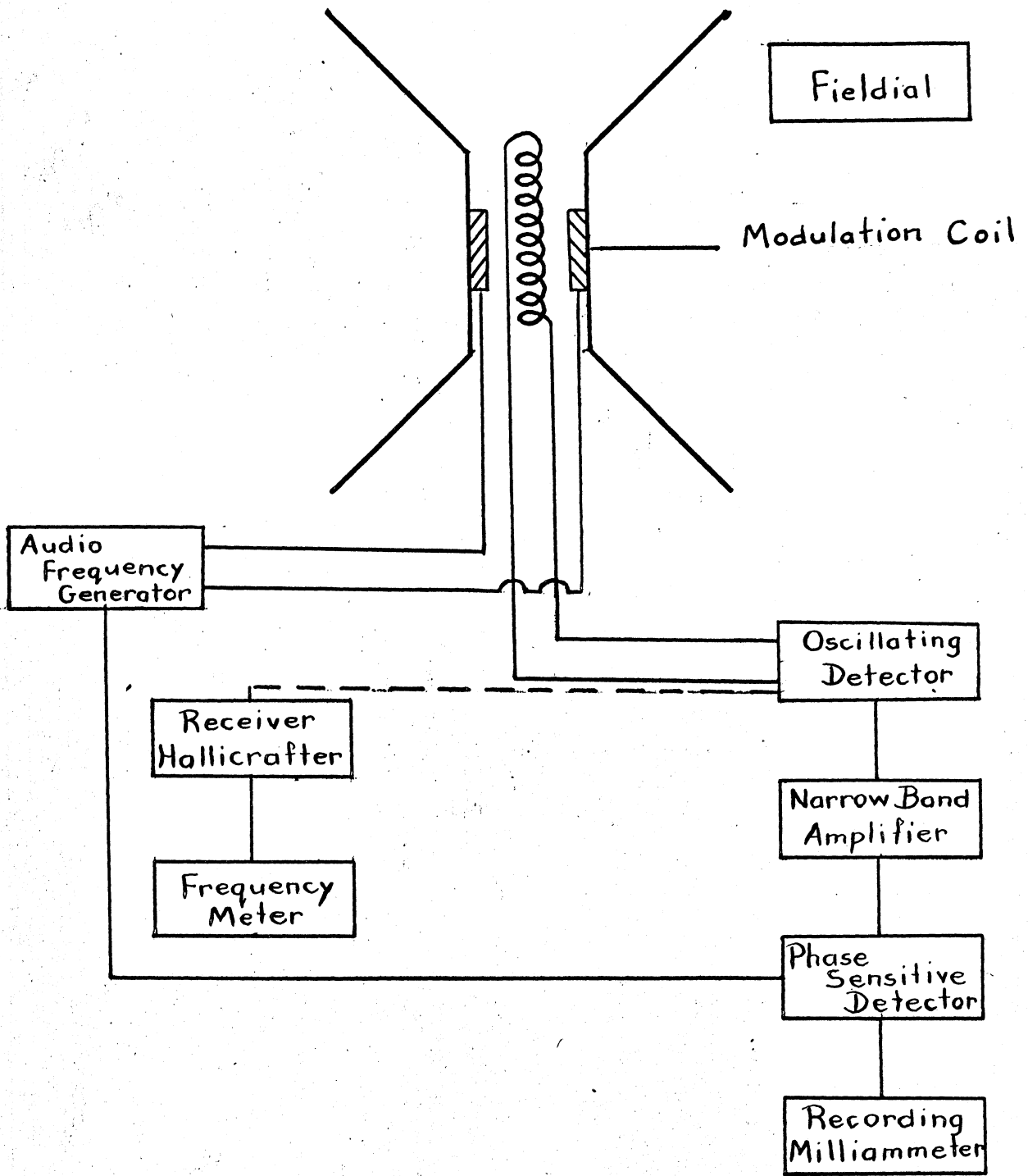
The arrangement of oxygen atoms around O_4 .

APPARATUS AND EXPERIMENTAL ARRANGEMENT(a) Absorption Experiment

The magnetic field was produced by a 12" Varian electromagnet monitored by a Varian V-FR2503 Fieldial. The block diagram of the NMR spectrometer is shown in Figure 5. The oscillating detector consists essentially of a marginal oscillator, a radio frequency amplifier, a detector and a wide band audio frequency amplifier. The resonating circuit of the marginal oscillator consists of a sample coil located in a sample holder which is fixed between a pair of Helmholtz coils. The frequency of the marginal oscillator is fixed. The field can be swept by variable amounts with the help of the Fieldial. The Helmholtz coils were energized by 200 c/sec. alternating current supplied by the audio frequency oscillator. The other parts of the spectrometer are a narrow-band amplifier tuned to 200 c/sec., a phase-sensitive detector and a recording milliammeter. The frequency is measured with the aid of a Hallicrafter Radio and a General Radio heterodyne frequency meter.

The spectrometer functions as follows: the Helmholtz coils modulate the external magnetic field with an amplitude much smaller (approximately 1/10) than the linewidth of the NMR signal. The resonance condition for the nuclei inside the sample coil, which manifests itself as a potential drop across the coil, is thus made repetitive at the modulating frequency. The signal, after radio-frequency amplification, is detected and then fed to the wide-band audio-frequency amplifier, the narrow-band audio-frequency amplifier and finally to the phase sensitive detector which produces a D.C. signal approximately proportional to the first derivative of the absorption curve. The D.C. signal is plotted on the

FIGURE 5
BLOCK DIAGRAM OF THE ABSORPTION SPECTROMETER



recording milliammeter.

(b) Nuclear Spin-Lattice Relaxation Study

The resonance condition may be approached slowly or rapidly. In the latter case, transient motions of the magnetic moment vector are set up which eventually decay to steady state motion in a time determined by the relaxation constants T_1 and T_2 . The study of transients gives a method of determining in a straightforward manner data on the relaxation constants T_1 and T_2 .

The sample under investigation is placed in an applied magnetic field consisting of two components: a steady component of magnitude H_0 oriented in the z direction and an oscillating component $2H_1 \cos \omega t$ in the x direction. As is well known, the oscillating component can be further decomposed into two circularly polarized components in the x - y plane rotating in opposite directions about the z axis. Only one of these, namely, that one rotating in the same sense as the free Larmor precession of the nuclear moment, is effective in changing the orientation of the nuclear moment; the other can be ignored. The resultant moment M of the sample may be resolved into three components: M_z along the z direction, u parallel to the effective rotating component of magnetic field and v orthogonal to M_z and leading the effective rotating field component by $\pi/2$ radians. The time dependence of these three components is given by the three Bloch (Torrey, 1949) differential equations.

The transient situation may be set up by any approach to resonant condition which is fast compared to the nutation time $1/\gamma H_1$. To do this any one of the three external parameters H_0 , H_1 or ω may be varied with

time in the form of a pulse starting at $t = 0$.

The pulse technique lends itself readily to a direct and straight forward measurement of the spin-lattice relaxation time T_1 . Suppose that H_1 is large enough to satisfy

$$\gamma H_1 \gg 1/T_2$$

or in other words the nutation time should be short compared to the relaxation times so that the inversion of the magnetization is adiabatic.

In this case the solution of the Bloch equation at resonance is

$$M_z/M_0 = m_0 \exp \left[-1/2 \left(\frac{1}{T_1} + \frac{1}{T_2} \right) t \right] \left[\cos \delta + \left(\frac{\beta - \alpha}{2} \right) \sin \delta \right] + 0 \quad (\alpha \beta)$$

where $M_0 = \chi_0 H_0$ χ_0 = static susceptibility

m_0 = initial value of M_z/M_0

$$\delta = \gamma H_1 t$$

$$\beta = 1/\gamma H_1 T_2$$

$$\alpha = 1/\gamma H_1 T_1$$

If the pulse duration is long compared with time $2T_1 T_2 / (T_1 + T_2)$, then the final value of M_z will be small compared with M_0 . In other words, the sample is almost completely demagnetized. During the interval between pulses, the sample will regain some of its magnetization because of the relaxation process. Hence, if $m_0 = M_z/M_0$ is the value at the beginning of the pulse, then

$$m_0 = 1 - \exp^{-t'/T_1}, \quad t' = \text{time between pulses} \quad (3)$$

If $m_0 \approx 1$, then according to the Bloch theory, v becomes proportional to m_0 . Hence, by observing the dependence of the initial amplitude of v as a function of time t' , and making use of Equation (3), T_1 can be directly obtained.

Two methods were used: Two-Pulse Method and One-Pulse Method. In the former, one obtains that for two 90° pulses separated by a time t' , the induced signal after the second pulse is proportional to $1 - \exp(-t'/T_1)$. In the latter, one obtains that for 90° pulses repeated every p seconds, the induced signal is proportional to $1 - \exp(-p/T_1)$. An example of the One-Pulse Method is given in Figures 10 and 11.

(c) The Effect of Inhomogeneities in H_1 and H_0

The effect of inhomogeneities in H_1 or H_0 is a distribution of nutational frequencies over the sample. The signal from the whole sample can be thought of as a superposition of signals from the various parts of the sample, each part being in an essentially homogeneous field. Signals from the various parts will differ somewhat in frequency because of the variation of $\omega_0 = \gamma H_0$ over the sample. Since they start out all in phase, the initial integrated amplitude is large, but after a few oscillations, phase differences develop which dampen the resultant signal.

The nutational frequency is given by

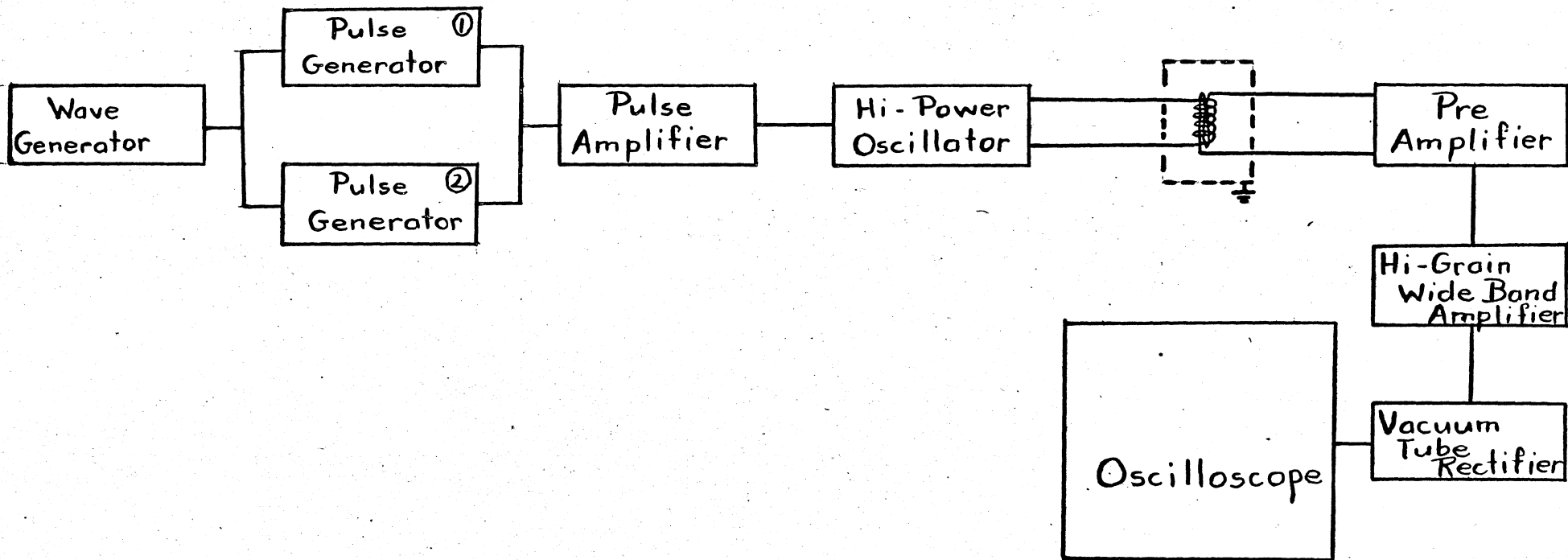
$$\Omega = (\gamma^2 H_1^2 + (\gamma H_0 - \omega)^2)^{1/2}$$

Now the nutational frequency at resonance is $\gamma H_1/2\pi$. Hence, an inhomogeneity in H_1 of ΔH_1 will cause an appreciable damping in a time of order $1/\Delta H_1$.

Now the nutational frequency at resonance does not depend on H_0 . Hence, if H_1 is large compared to the inhomogeneity in H_0 , there will be little variation of Ω over the sample. However, it does not pay to increase H_1 indefinitely, but only until the effect of inhomogeneity in H_1 is about that of H_0 . The inhomogeneity in H_1 can be considerably reduced (at the expense of signal strength) by concentrating the sample near the centre of the r.f. coil.

The experimental arrangement of the T_1 spectrometer is given in Figure 6. The nuclear resonance pulse apparatus is a version of the equipment originally described by Mansfield and Powles (1963). It is capable of giving 25 gauss pulses at 30 mc/sec. The 90° pulse length is approximately 2μ sec. in a 9 mm I.D. coil. The pulse has a very rapid rise and fall time. The spectrometer has a fast recovery time and high gain receiver, which allows the nuclear signal to be read 5μ sec. after the pulse was applied. It produces the following pulse sequences: $90^\circ, \tau, 180^\circ$; and $90^\circ, \tau, 90^\circ, \dots$, where τ is the pulse separation from 1 m sec. upward.

FIGURE 6
BLOCK DIAGRAM OF T₁ SPECTROMETER



EXPERIMENTAL PROCEDURE AND RESULTS

The proton resonance spectrum of hydrated gallium sulfate was recorded at -268°C and at intervals of approximately 20°C over the temperature range -196°C to $+90^{\circ}\text{C}$. Sample absorption derivative curves obtained at -268°C and at $+22^{\circ}\text{C}$ are shown in Figures 7 and 8, respectively. At the higher temperatures, the derivative curves indicated a rather broad bell-shaped absorption peak with little evidence of structure. The extrema of the derivative curve are separated by 6.6 gauss which remained constant throughout the entire temperature range which was studied. At -268°C , Figure 7, the signal is broadened by "tails" which develop at the extremities of the signal and there is some indication of peaking of these tails at approximately 10 gauss from the centre of the spectrum.

The second moment of the proton signal was calculated using a computer program from the experimentally measured derivative of the absorption curve. Corrections were made for modulation broadening using the formula given by Andrews (1953) and for inhomogeneity broadening. The latter was made by comparing the signals obtained under identical experimental conditions with the magnet used in this work and a high resolution magnet in which the inhomogeneity is negligible. A plot of the second moment as a function of temperature is shown in Figure 9. The second moment increases slowly from $5.5 \pm 0.4 \text{ gauss}^2$ to $6.3 \pm 0.5 \text{ gauss}^2$ as the temperature is decreased from $+90^{\circ}\text{C}$ to -170°C and then increases abruptly to $10.6 \pm 0.8 \text{ gauss}^2$ at -196°C . Unfortunately, the experimental apparatus did not permit data to be collected in the temperature range below -196°C except at liquid helium temperature where the second moment was $15.3 \pm 1.2 \text{ gauss}^2$.

FIGURE 7
ABSORPTION DERIVATIVE CURVE AT -268°C

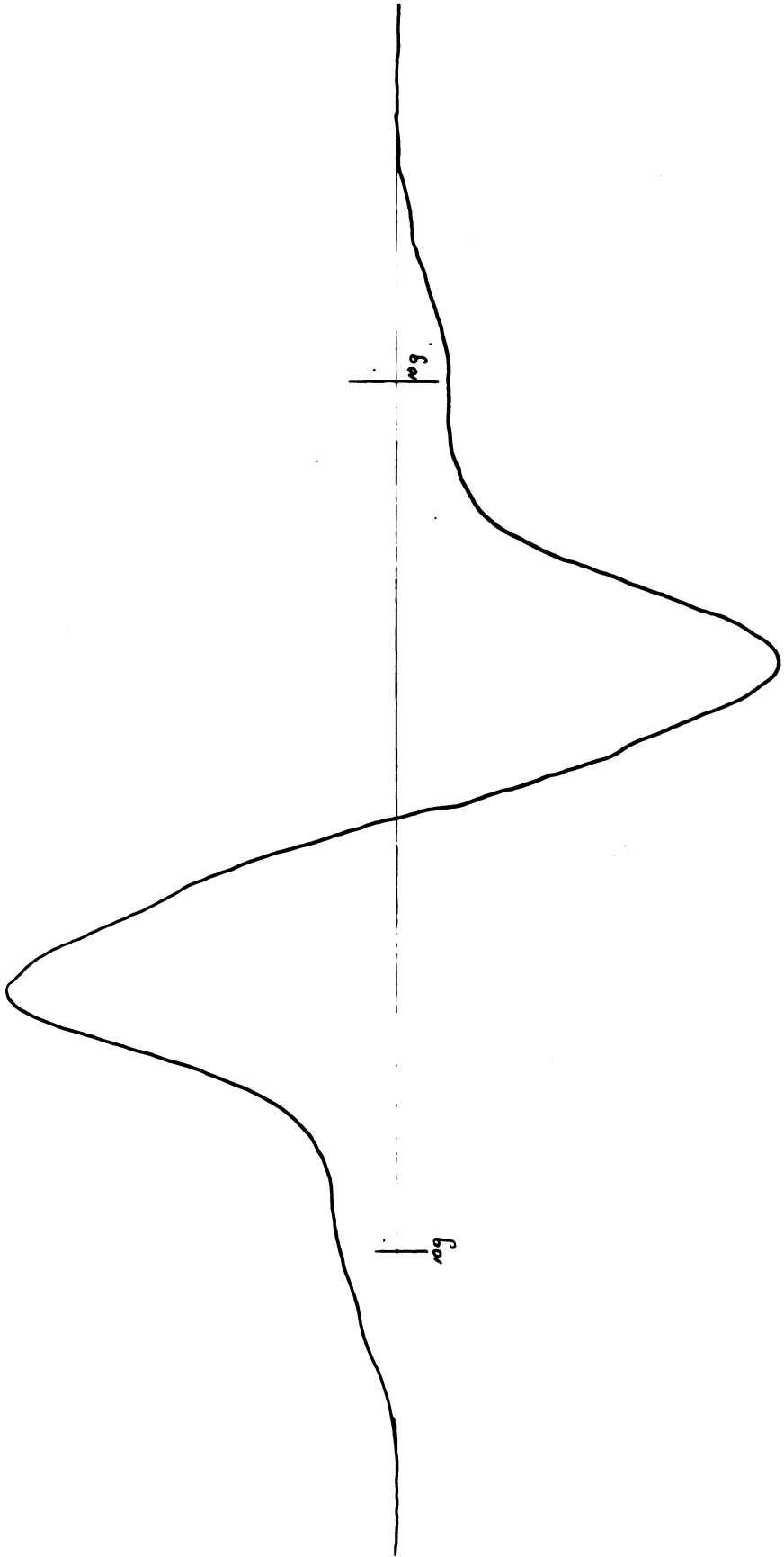


FIGURE 8
ABSORPTION DERIVATIVE CURVE AT +22°C

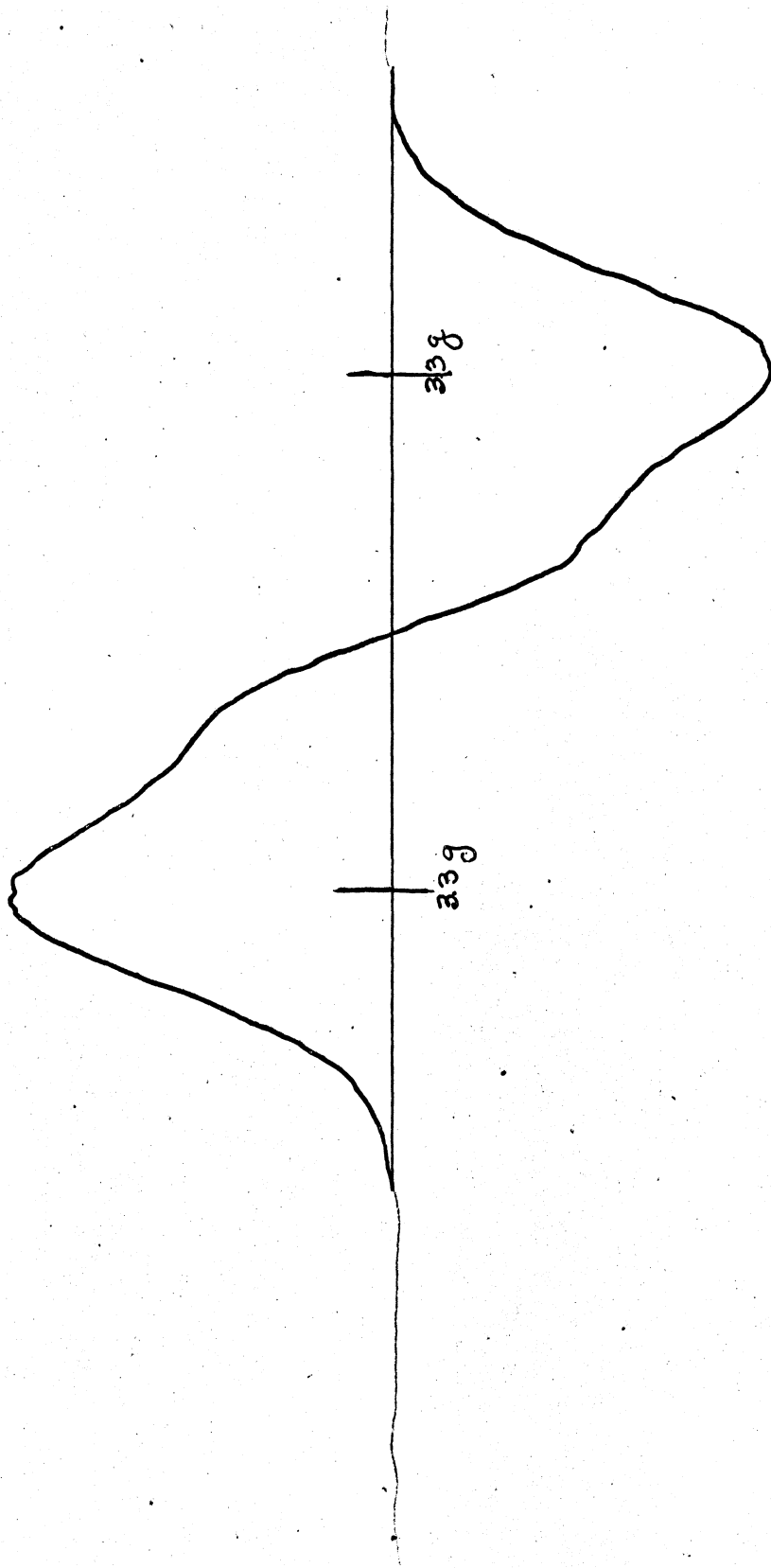
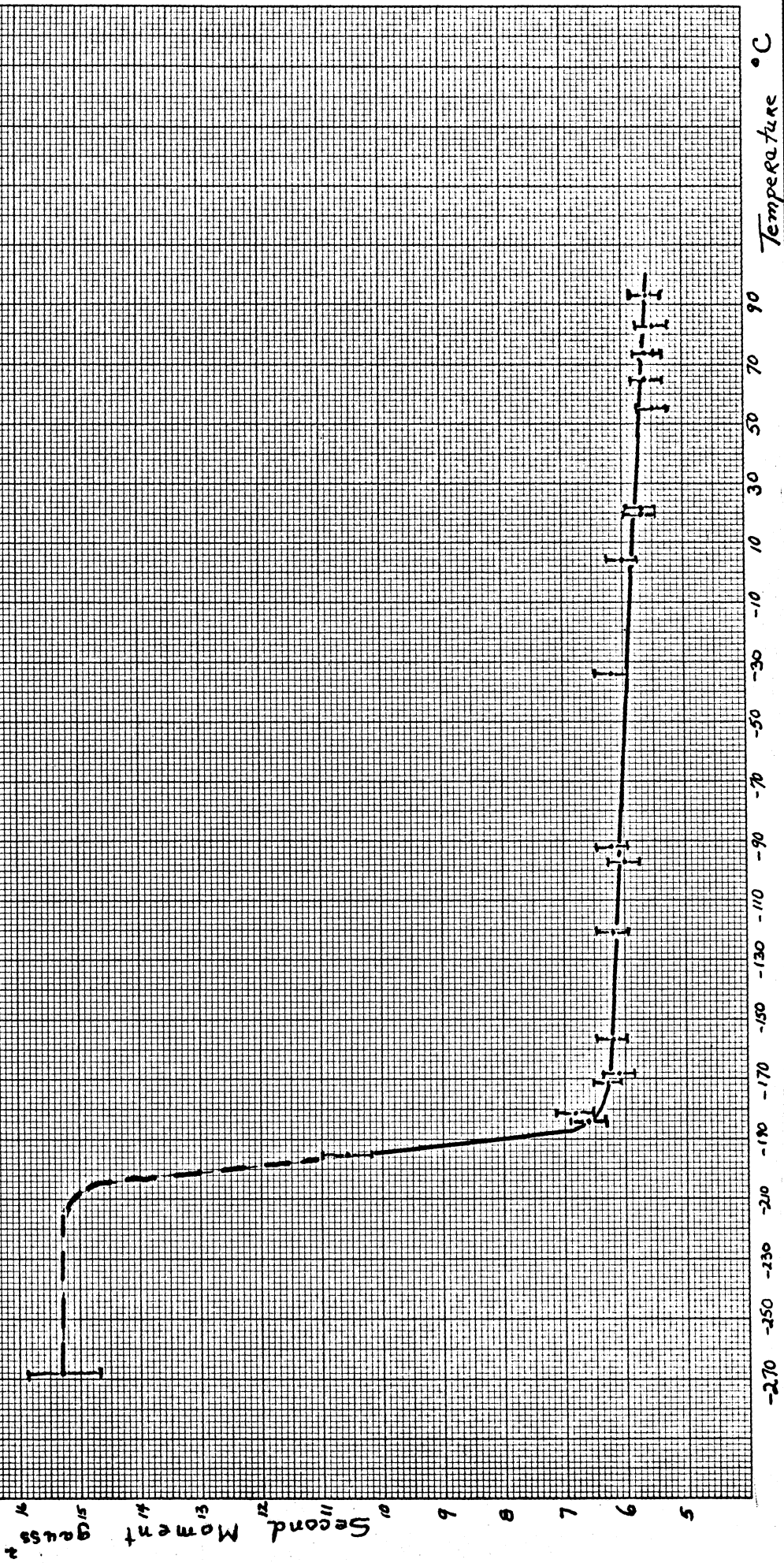


FIGURE 9
TEMPERATURE DEPENDENCE OF SECOND MOMENT



Temperature °C

Second Moment Gauss²

An approximate value of the activation energy associated with a transition may be obtained using the formula $E_a = 37T_c$ (Waugh, 1963) where T_c is the temperature at which the linewidth begins to decrease. Since we were unable to follow the entire temperature dependence of the transition it was necessary to estimate T_c by assuming a symmetric temperature dependence in the second moment curve at the transition. This rough approximation gave -213°C and 2.2 ± 0.2 kcal/mole for T_c and E_a , respectively.

Transient experiments were carried out at selected temperatures over the range from $+22^\circ\text{C}$ to -170°C and all experimental results were photographically recorded. For each temperature, both the two-pulse method and the one-pulse method were used. A typical result showing the signal decaying with time is given in Figure 10. The induced signal intensity against pulse separation time was plotted for each set of such data. A typical result can be seen in Figure 11. Finally, T_1 was plotted versus $1/T$ as shown in Figure 12. This curve shows a BPP minimum at about -146°C . The temperature corresponding to the minimum in this curve was obtained by extending the straight lines on either side of BPP minimum and obtaining the intersection. The value of the activation energy obtained from the slope of the temperature high-side is 1.95 ± 0.2 kcal/mole. By applying the condition at the BPP minimum ($\omega\tau_c = .616$) it was found that the corresponding transition temperature, T_c , is approximately -206°C . A compilation of data is given in Table II.

At higher temperatures, beginning at about -70°C , T_1 again begins to decrease. Whatever it is that is producing this decrease does not affect the proton second moment which decreases very slowly over the

FIGURE 10
PHOTOGRAPH OF RELAXATION SIGNAL AT -138°C

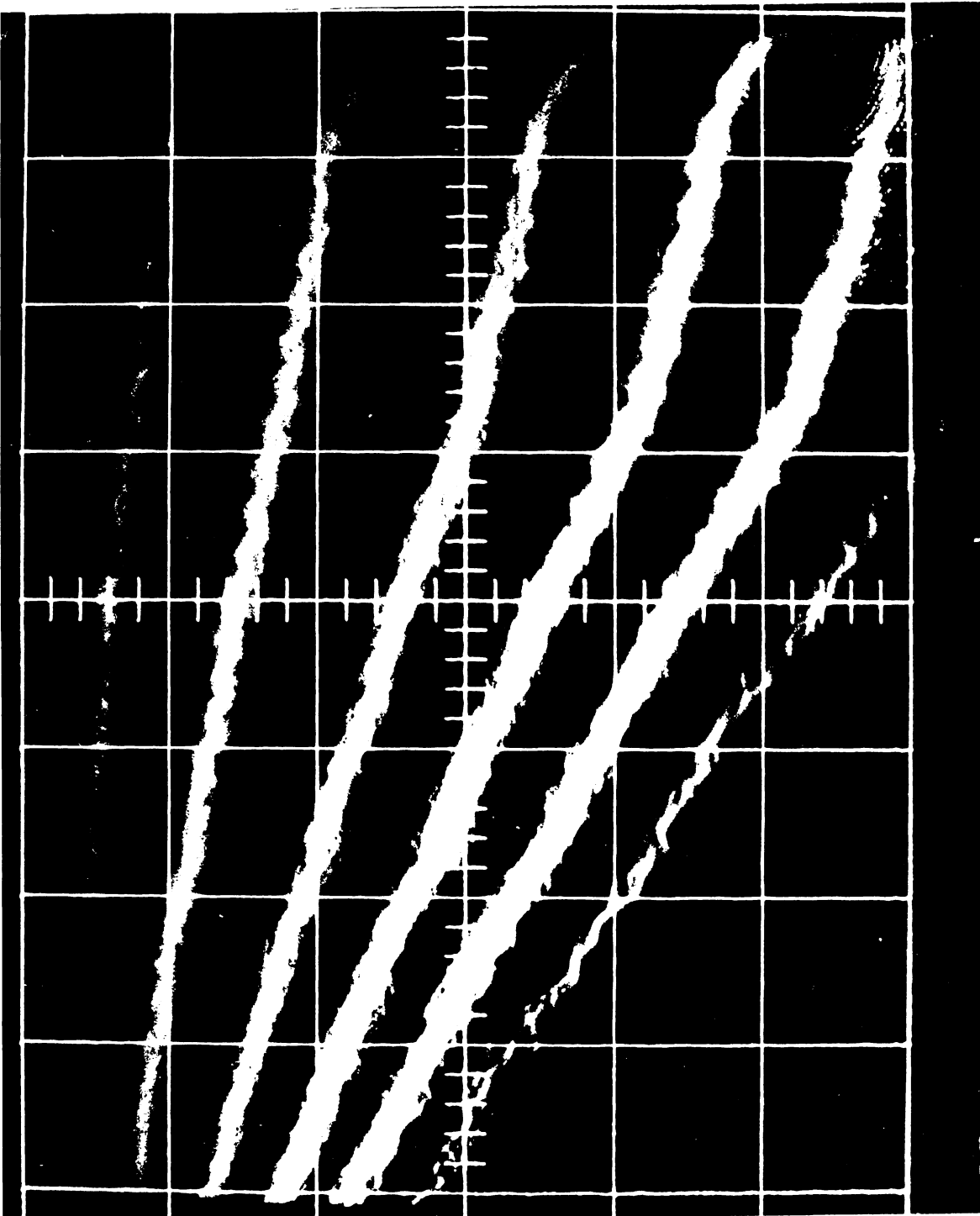
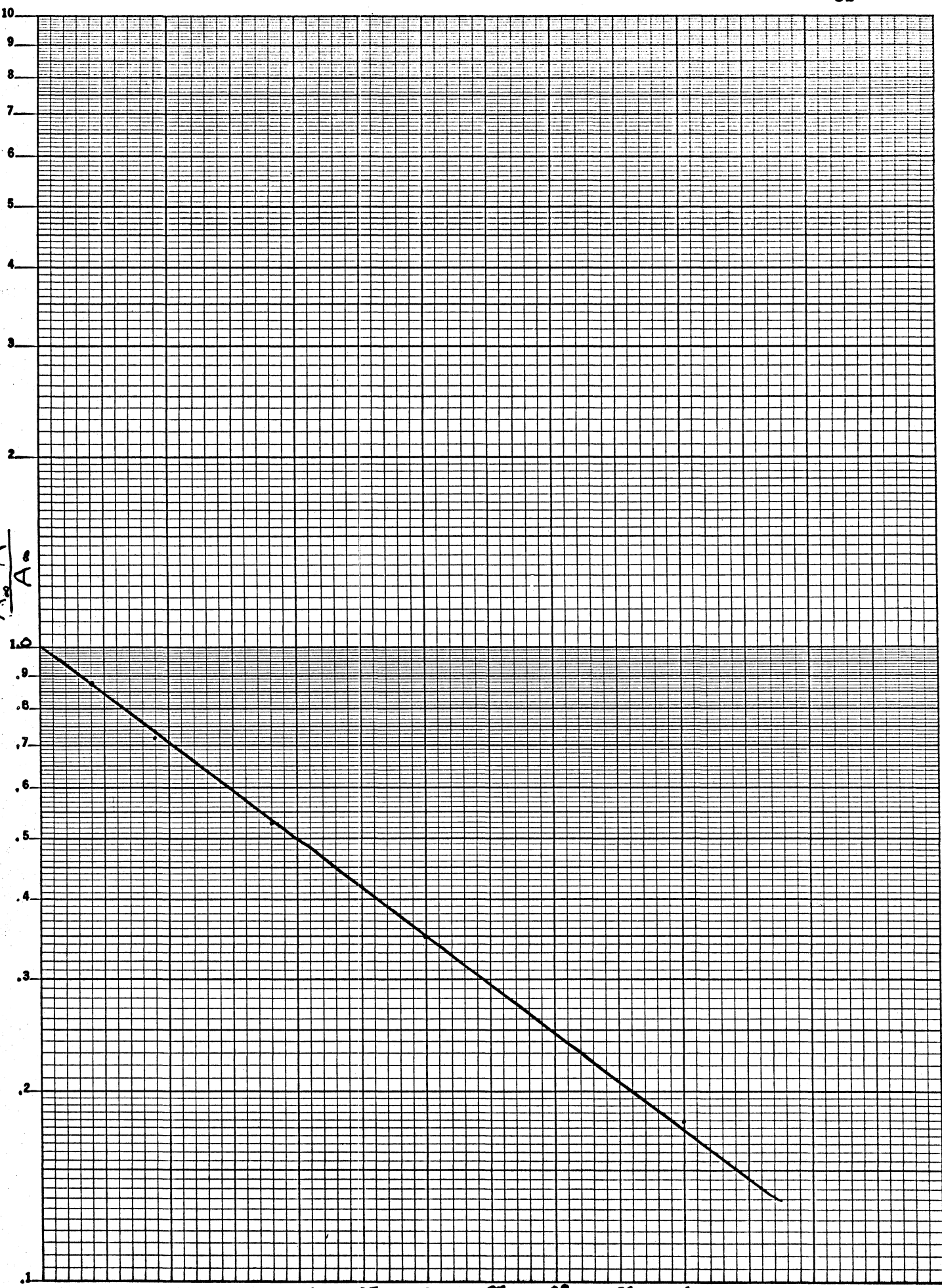


FIGURE 11**TIME DEPENDENCE OF INDUCED SIGNAL****Temp -138°C** **The slope yields: $T_1 = 0.06 \text{ sec}$**

TYPE 2 CYCLES X 70 DIVISIONS MADE IN U.S.A.
KEUFFEL & ESSER CO.

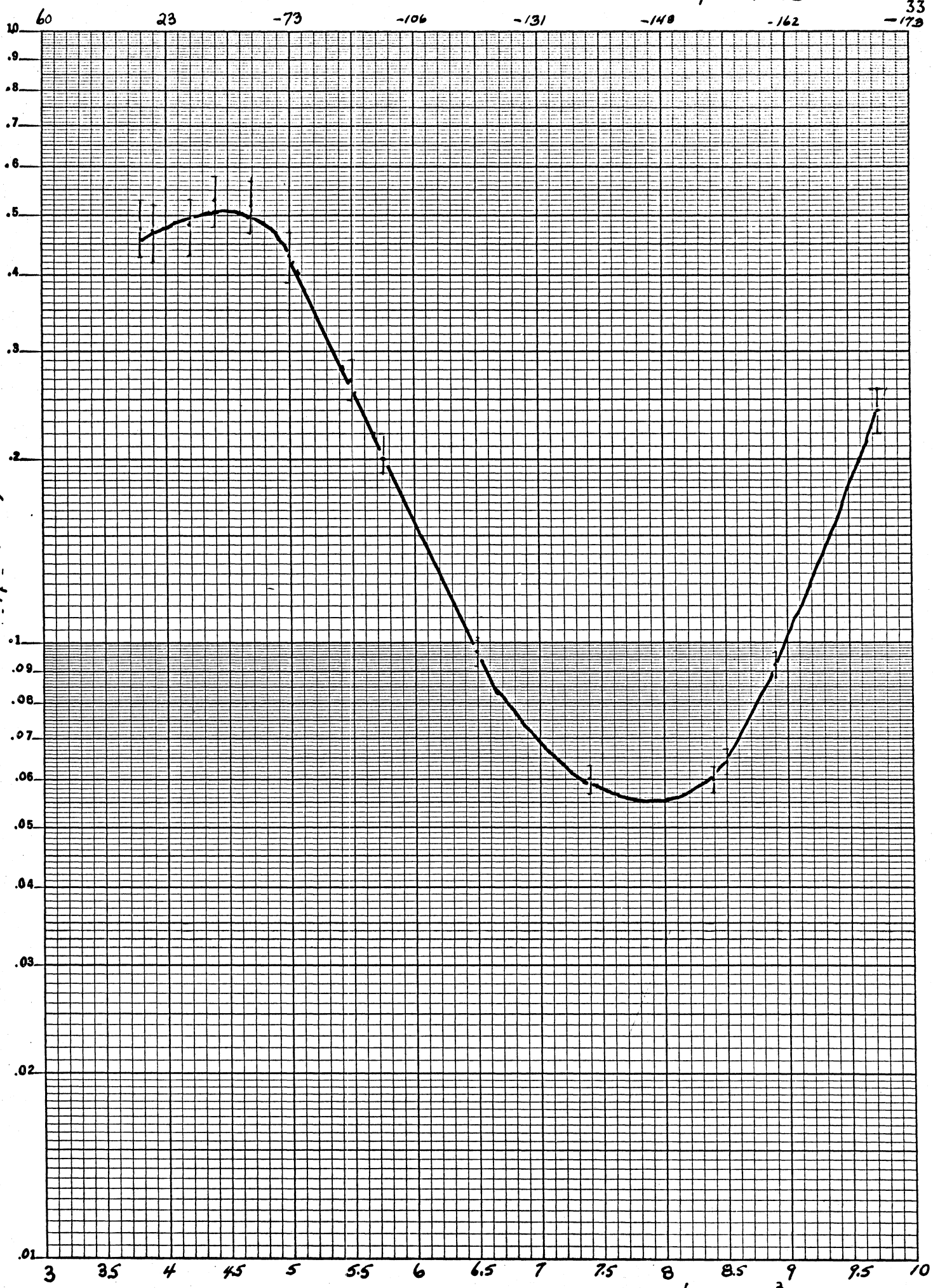
$$\frac{A_0 - A}{A_0}$$



Time (sec)

FIGURE 12
TEMPERATURE DEPENDENCE OF T_1

Temperature °C
33
-173



$1/T$ (sec)

$1/T \text{ (K} \times 10^3)$

11 1/2 INCHES X 7 1/2 DIVISIONS MADE IN U.S.A.
KEUFFEL & ESSER CO.

TABLE II
TABULATION OF RESULTS

Absorption Method

Second Moment (rigid lattice):	$15.3 \pm 1.2 \text{ gauss}^2$
Second Moment (above transition):	$6.0 \pm 0.5 \text{ gauss}^2$
Transition Temperature:	$T_c = 60 \pm 10^\circ\text{K}$
Activation Energy:	$E_a = 2.2 \pm 0.2 \text{ kcal/mole}$

Transient Method

Temperature of BPP minimum:	$T_{\min} = 127 \pm 5^\circ\text{K}$
Correlation Frequency:	$\nu_{oc} = 12.6 \times 10^{10} \text{ c/sec.}$
Larmor Precession Frequency:	$\nu_L = 29 \text{ mc/s}$
Transition Temperature:	$T_c = 67 \pm 5^\circ\text{K}$
Activation Energy:	$E_a = 1.95 \pm 0.2 \text{ kcal/mole}$

temperature range from -170° to $+90^{\circ}\text{C}$. Further studies of T_1 at higher temperatures will be needed to clarify this effect.

The linearity of the pulse spectrometer was checked with the aid of a General Radio Standard Signal Generator, Model 1001-A. All corrections have been included in the above mentioned data.

DISCUSSION

The contraction of a crystal as it is cooled is expected to produce an increase in the proton second moment because the interproton distances are reduced. Assuming the reasonable value of $9.5 \times 10^{-6} \text{ deg}^{-1}$ for the linear expansion coefficient of hydrated gallium sulfate, one would expect an increase in the second moment of approximately 1 gauss^2 as the crystal is cooled through 260°C . This compares well with the increase of 1.1 gauss^2 which was observed as the crystal was cooled from $+90^\circ\text{C}$ to -170°C .

The abrupt change in the value of proton second moment between -180°C and -220°C is caused by a molecular group containing hydrogen atoms which is capable of hindered rotation or reorientation at these low temperatures. Neglecting the normal lattice vibrations, the structure is effectively rigid below -220°C but as it is heated above this temperature, the molecular group begins to reorient producing a rapid narrowing of the proton resonance. Conversely, if the crystal is cooled below -180°C , the motion begins to freeze-out leading to a rapid increase in the second moment. Such a motion would be expected to strongly effect the spin relaxation time as well and, indeed, a deep minimum in the T_1 versus T curve was observed at -146°C .

The nature of the molecular group causing the line-width transition is related to the primary question as to the existence of the oxonium ion H_3O^+ and can be expected to throw some light on this question. The likely alternatives for the structural formula of hydrated gallium sulfate are (a) $(\text{H}_3\text{O})\text{Ga}_3(\text{OH})_6(\text{SO}_4)_2$, (b) $\text{H Ga}_3(\text{OH})_6(\text{SO}_4)_2 \cdot \text{H}_2\text{O}$, and (c) $\text{Ga}_3 \{(\text{OH})_5\text{H}_2\text{O}\} \text{SO}_4 \cdot \text{H}_2\text{O}$. The alternatives (b) and (c) are essentially

the same but (b) is intended to represent the possibility that the acid hydrogen is relatively isolated from the other hydrogen atoms whereas in (c) the acid hydrogen is associated with the hydroxyl groups on a statistical basis to form a water molecule. The molecular groups subject to molecular reorientation are therefore either the H_3O^+ ions or the H_2O molecules.

The value of the activation energy, 2 kcal/mole, is very low but well within the range one would expect for an H_3O^+ ion in the highly symmetrical site available in gallium sulfate. On the other hand, it seems to be much too low for reorientation of a water molecule for which the activation energy is expected to be more than 6 kcal/mole.

One also must account for the change of 9.1 gauss² observed in the linewidth transition. To produce a change of this magnitude, all the rotating groups' intramolecular contribution to the second moment must vanish. To produce a change of 9.1 gauss², an oxonium ion which would contain one-third of the protons in gallium sulfate, would have to have an unweighted second moment of 27.3 gauss². From this value of the second moment we obtain, for the interproton distance in the H_3O^+ ion, the very reasonable value of 1.72Å. This is in good agreement with the value 1.71Å (Kakiuchi et al., 1952) observed for hydrogen perchlorate monohydrate. On the other hand, if we assume a normal interproton distance of 1.59Å for the water molecules, alternative (b) can produce a change of only 5 gauss² in the second moment which effectively rules it out. Although it is conceivable that alternative (c) could produce a change of 10 gauss² in the second moment, it is extremely unlikely. This is so because the change of 10 gauss² would require two water molecules in quite different

surroundings to have almost exactly the same activation energy. It would also require reorientation about three non-coplanar axes and this is very unlikely for the statistically associated water molecule. It is apparent that H_3O^+ ions can account quite satisfactorily for the features exhibited by the transition. There is, however, a difficulty remaining which has yet to be resolved.

If we now begin with rigid lattice value of second moment and subtract the contributions of H_3O^+ of 9.1 gauss^2 and an intermolecular broadening of about 2 gauss^2 we are left with a residual second moment of 4.2 gauss^2 . This gives an unweighted value of 6.3 gauss^2 which must be due to the hydroxyls. However, the value of 6.3 gauss^2 is too large to be due to isolated hydroxyls, the second moment of which is at most 2 or 3 gauss^2 . The hydroxyls must exist in groups. The structure does not permit the formation of pairs. A possible alternative is that the protons exist in groups of three bonding the three O_3 to O_1 . A calculation using Johansson's interatomic distances yields a proton-proton separation of 2.9\AA . This is much too large a separation to account for a second moment of 6.3 gauss^2 . An interproton distance of 2.2\AA would be needed to account for 6.6 gauss^2 . Another possibility is that the sample is highly contaminated by a paramagnetic impurity, thus broadening the signal. This unexpected contribution to the second moment by the hydroxyl hydrogens remains as an unexplained and tantalizing problem. A further attempt will be made to clarify it.

BIBLIOGRAPHY

- Andrews, E. R., 1953, Phys. Rev., 91, 425.
- Bloembergen, N., Purcell, E. M., and Pound, R. V., 1948, Phys. Rev., 73; 679.
- Conway, B. E., Bockris, J., and Linton, H., 1956, J. Chem. Phys., 24, 834.
- Hendricks, S. B., 1937, Am. Mineral., 22, 773.
- Johansson, G., 1962, Ark. Kemi, 20, 343.
- Kakiuchi, Y., Shono, H., Komatsu, H., and Kigoshi, K., 1952, J. Phy. Soc. Japan, 7, 102.
- Mansfield, P., and Powles, J. G., 1963, J. Sci. Instrum., 40, 232.
- Purcell, E. M., Torrey, H. C., and Pound, R. V., 1946, Phys. Rev., 69, 37.
- Shiskin, N. V., 1948, Sci. Reports Saratov State University.
- Torrey, H. C., 1949, Phys. Rev., 76, 1059.
- Van Vleck, J. H., 1948, Phys. Rev., 74, 1168.
- Waugh, J. S., and Fedin, E. I., 1963, Soviet Phys. Sol. State, 4, 1633.